Citation: Molecular Therapy—Nucleic Acids (2013) 2, e112; doi:10.1038/mtna.2013.39

www.nature.com/mtna

Targeted Myostatin Gene Editing in Multiple Mammalian Species Directed by a Single Pair of TALE Nucleases

Li Xu[1], Piming Zhao[1], Andrew Mariano[1] and Renzhi Han[1]

Myostatin (MSTN) is a negative regulator of skeletal muscle mass. Strategies to block myostatin signaling pathway have been extensively pursued to increase muscle mass in various disease settings including muscular dystrophy. Here, we report a new class of reagents based on transcription activator-like effector nucleases (TALENs) to disrupt myostatin expression at the genome level. We designed a pair of MSTN TALENs to target a highly conserved sequence in the coding region of the myostatin gene. We demonstrate that codelivery of these MSTN TALENs induce highly specific and efficient gene disruption in a variety of human, cattle, and mouse cells. Based upon sequence analysis, this pair of TALENs is expected to be functional in many other mammalian species. Moreover, we demonstrate that these MSTN TALENs can facilitate targeted integration of a mCherry expression cassette or a larger muscular dystrophy gene (dysferlin) expression cassette into the *MSTN* locus in mouse or human cells. Therefore, targeted editing of the myostatin gene using our highly specific and efficient TALEN pair would facilitate cell engineering, allowing potential use in translational research for cell-based therapy.

Molecular Therapy—Nucleic Acids (2013) **2**, e112; doi:10.1038/mtna.2013.39; published online 30 July 2013
Subject Category: Gene insertion, deletion & modification

Introduction

Myostatin (MSTN) is a transforming growth factor-β family member that plays a critical role in negatively regulating skeletal muscle mass.[1] Genetic studies have demonstrated that myostatin gene deficiency leads to muscle hypertrophy due to a combination of increased fiber numbers and increased fiber sizes in multiple species including human,[2] cattle,[3–5] mouse,[1] sheep,[6] and dog[7] without causing severe adverse consequences. Therefore, extensive efforts have been undertaken to develop effective strategies for blocking the myostatin signaling pathway as therapies for various muscle-wasting diseases such as muscular dystrophy, sarcopenia, and long bedding patients.[8–12] Indeed, myostatin inhibitors have shown great promise to significantly increase muscle growth in model animals.[9,13–16]

Targeting the *MSTN* gene would provide a permanent solution to block myostatin signaling. However, conventional gene targeting approach has been limited to mouse embryonic stem cells and not readily adaptable for most other cell types because of the extremely low targeting frequency. Recent studies have shown that targeted genome editing with minimal toxicity in many different types of cells is possible by combining engineered zinc finger nucleases (ZFNs) with inherent DNA repair mechanisms within the cell.[17] It has been shown that ZFNs promote genome editing via nonhomologous end-joining (NHEJ) and homology-directed DNA repair by creating a double-strand break at a specific target locus.[18] A typical nuclease is composed of two essential domains: the DNA-binding domain and the nonspecific cleavage domain of the FokI restriction enzyme. The DNA-binding domain, which is composed of multiple zinc finger arrays, can be re-engineered to bind to a wide variety of DNA sequences, making it possible to engineer ZFNs which specifically target the user-defined sequences. ZFN-facilitated genome editing allows stable integration of therapeutic genes or restoration of mutated genes in specific genetic loci.[19] It thus offers a promising approach for treating genetic disorders and has gained much research interest recently. Since the first seminal publications about ZFNs in the late 1990s,[18,20,21] many ZFNs have been successfully engineered to perform genome editing in cells of several different species, including human and mouse. ZFN-mediated *in vivo* genome editing was recently shown to restore hemostasis in a mouse model of hemophilia via adeno-associated virus-mediated delivery of ZFNs and a donor gene into the mouse liver,[22] and ZFN-mediated CCR5 gene knockout is currently in clinical trial for establishing HIV-1 resistance in $CD4^+$ T cells.[23] These exciting progresses raise the possibility of genome editing as a viable strategy to treat diseases caused by genetic mutation. However, there is still a lack of an optimal strategy to engineering highly active and specific ZFNs.

Recently, a new class of nucleases called transcription activator-like effector nucleases (TALENs), which contain DNA-binding domains based on transcription activator-like effector (TALE) proteins from *Xanthomonas* plant pathogens, have emerged.[24–27] The central repeat domain in the TALE structure mediates DNA binding with each repeat specifying one target base. The base preference of each repeat is determined by two critical, adjacent amino acids referred to as the "repeat variable di-residue" (RVD) which preferentially recognizes one of the four bases in the target site.[28,29] This simple "two amino acids for one base" code enables rapid engineering of customized TALE repeat arrays that recognize a user-defined target sequence. It has been shown that unique TALE-binding sites can be found on average every 35 base pairs,[27] making it highly attractive for scientific laboratories to practice gene editing in various cell types.

[1]Department of Cell and Molecular Physiology, Loyola University Chicago Health Science Division, Maywood, Illinois. Correspondence: Renzhi Han, Department of Cell and Molecular Physiology, Loyola University Chicago Health Science Division, Maywood, Illinois. E-mail: renhan@lumc.edu
Keywords: dysferlin; gene editing; myostatin; TALEN
Received 18 January 2013; accepted 12 June 2013; advance online publication 30 July 2013. doi:10.1038/mtna.2013.39

In this study, we report the successful engineering of a TALEN pair designed to target a highly conserved sequence within the coding region of the *MSTN* gene. High rates of *MSTN* mutations and targeted DNA addition were efficiently induced by the TALEN pair in various cell lines of multiple species.

Results

Design and characterization of MSTN TALEN

To design a working TALEN for editing human *MSTN* gene, we analyzed the sequence within exon 2 through the online TALEN Targeter program (https://talent.cac.cornell.edu/node/add/talen)[27,30] and selected a potential target site (**Figure 1a**). We assembled the TALEN pair using the Golden Gate Platform as described previously[27] in two separate plasmids, each with a WT FokI domain and expression driven by a CMV promoter. Transfection of each of these TALENs (GDF8-L or GDF8-R) into HEK293 cells did not result in any detectable gene editing activity as measured by T7E1-directed mismatch cleavage assay[31] which detects TALEN pair-induced NHEJ-mediated small insertions or deletions (indels) (**Figure 1b**). However, cotransfection of the TALEN pair efficiently induced indels which can be detected as two cleavage bands using T7E1 assay (**Figure 1b**). The frequency of mutated alleles is estimated to be ~19.6% based on the gel densitometry.

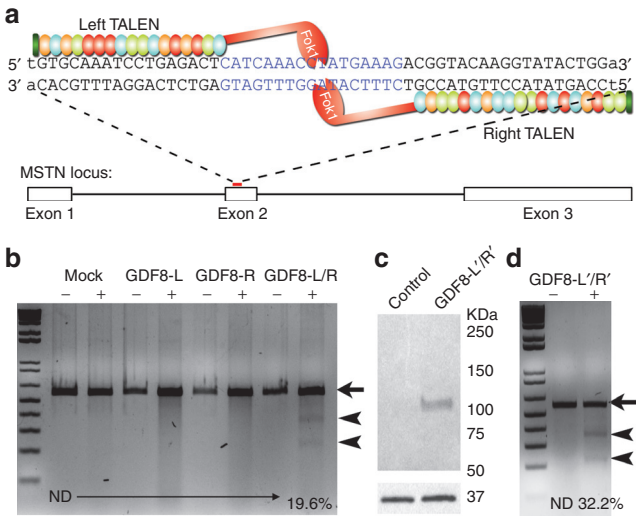

Figure 1 Construction of MSTN TALENs. (**a**) Schematic showing the design of MSTN TALENs. A TALEN is composed of a DNA binding domain and a nonspecific DNA cleavage domain (FokI). A pair of TALENs bind to opposite strands of a DNA double helix. The left and right target sites were located at the Exon 2 of human MSTN locus. (**b**) T7E1 assay of the gene-editing activity of the left (GDF8-L) and right (GDF8-R) TALENs with a wild-type FokI domain in human HEK293 cells. (**c**) 2A-mediated self-processing of the left and right TALEN monomers linked by a 2A peptide sequence, each harboring ELD-sharkey and KKR-sharkey variant of FokI domain, respectively (GDF8-L′/R′). The 110 kDa TALEN monomers were detected with a FLAG tag antibody. We could see only one band at 110 kDa because the two monomers have about the same size. GAPDH was used as a loading control. (**d**) T7E1 assay of the gene-editing activity of the GDF8-L′/R′. Data shown were representative of at least three experiments.

Previous studies demonstrated that WT FokI domain fused to zinc finger proteins can form homodimers and thus induce off-target activities and significant cellular toxicity.[32–37] To overcome this limitation, others have developed obligate heterodimer variants of the FokI cleavage domain, which greatly reduced the cellular toxicity of ZFNs.[32–37] Therefore, we also assembled the MSTN TALENs using two well-characterized obligate heterodimeric variants (Q486E, I499L, N496D in the left TALEN and E490K, I538K and H537R in the right TALEN)[34] to reduce homodimer formation. The "Sharkey" mutations S418P and K441E[32,37] were also introduced to both heterodimer FokI domains to further enhance cleavage activity. The complete sequences of both TALENs are provided in **Supplementary Figure S1 and Figure S2** online. The two TALENs were linked by a self-cleaving 2A peptide sequence,[38] which allows the transcription and translation of both TALENs at an equal molar ratio. Western blotting analysis confirmed faithful expression of the ~110kDa TALEN monomers (**Figure 1c**). To a very small extent, the 220 kDa full-length precursor protein was visible with a high exposure time (data not shown). Transfection of this TALENs-encoding plasmid resulted in a mutation frequency of ~32.2% (**Figure 1d**) in human HEK293 cells, significantly higher than that achieved with two separate TALEN monomer plasmids comprised of WT FokI domain. We used this plasmid throughout the following studies.

To examine the dependence of the mutation rate on time after TALEN treatment, we performed the T7E1 assay on HEK293 cells transfected with the TALEN plasmid at various time points post-transfection. Mutation events can be detected at 20 hours after transfection with the mutation frequency peaking at 32 hours and well maintained throughout 4 days post-transfection (**Figure 2a**). This trend is well correlated with the typical expression time course in a transient transfection experiment. To test whether TALENs-mediated mutations persist during long-period culture, we passaged a dish of transfected cells for six generations (total one month) and demonstrated that the mutations are maintained after a long period of culture (**Figure 2b**). These data suggest that the TALENs-mediated gene mutations are permanent and inheritable.

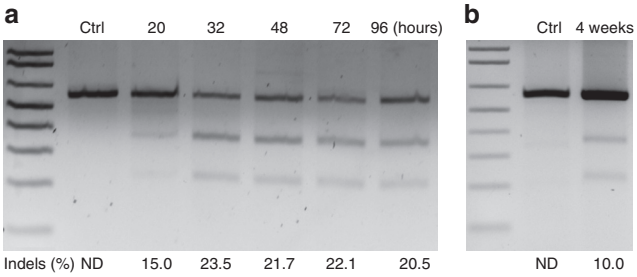

Figure 2 MSTN TALENs mediate long-lasting gene editing in HEK293 cells. (**a**) HEK293 cells were transfected with the plasmid encoding MSTN TALENs and analyzed by T7E1 assays at 20, 32, 48, 72, and 96 hours post-transfection. (**b**) A dish of HEK293 cells after transfection with the plasmid encoding MSTN TALENs were maintained in culture and passaged for six generations (total 1 month). The cells were then analyzed by T7E1 assay. Nontransfected HEK293 cells were used as control (Ctrl). ND, not detected. Data shown were representative of at least three experiments.

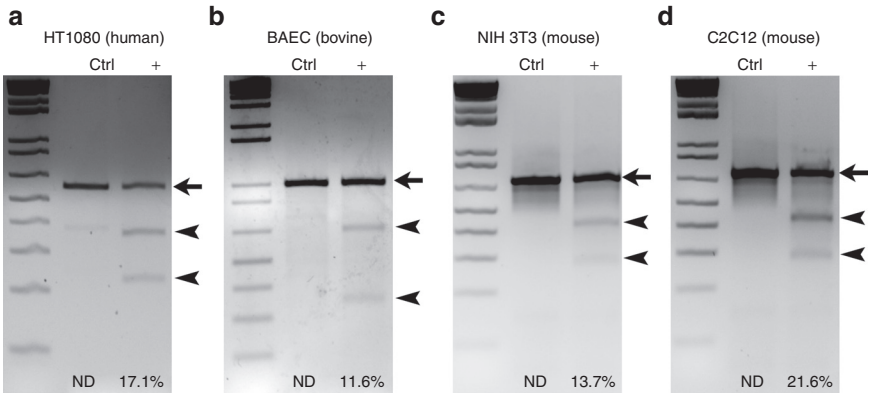

Figure 3 Gene-editing activities of MSTN TALENs in various cell lines of different species. Various human, bovine and mouse cell lines were co-transfected with the plasmid encoding the left and right TALENs linked by a self-cleaving 2A peptide sequence and analyzed by T7E1 assay 72 hours post-transfection. (**a**) HT1080: a human fibrosarcoma cell line; (**b**) bovine aortic endothelial cells (BAEC); (**c**) NIH 3T3: a mouse embryonic fibroblast cell line; (**d**) C2C12: a mouse myoblast cell line. Nontransfected cells were used as control (Ctrl). ND, not detected. Arrow heads indicate the two cleaved bands while the arrow indicates noncleaved band. Data shown were representative of at least three experiments.

Gene editing in other mammalian species using the same MSTN TALEN pair

Since the human target sequence of our MSTN TALENs is highly conserved among different mammalian species, and particularly is exactly the same in primates, several livestock animals and mice (see **Supplementary Figure S3** online), we reasoned that our MSTN TALENs are functional in cells of various species. To test this, we transfected the TALENs-expressing plasmid into several cell lines of different species including human HT1080 fibrosarcoma cells, bovine aortic endothelial cells (BAEC), mouse NIH 3T3 embryonic fibroblasts, and mouse C2C12 myoblasts. T7E1 assays performed on all human, bovine, and mouse cells demonstrated high efficiency of gene editing activities induced by this pair of TALENs (**Figure 3**). The mutation frequency varies from 11.6 to 21.6% among different cell lines.

The quantification of mutation frequency is likely underestimated since the transfection efficiency in most of the examined cell lines cannot reach 100%. To overcome the problem of low transfection efficiency, we added an EGFP fusion tag in the TALEN construct so that we can enrich positively-transfected NIH 3T3 cells by FACS. T7E1 assay showed that cell sorting increased the gene editing activity by about threefold (**Figure 4a**) (43.7% in sorted cells versus 13.7% in nonsorted cells shown in **Figure 3**), indicating that transfection efficiency is a critical factor in measuring gene editing activity. In addition to transfection efficiency, there are other factors, such as the gel densitometry sensitivity, that can influence the measured gene editing efficiency using the T7E1 assay. As an alternative approach to examine the mutation frequency induced by MSTN TALENs, we cloned the DNA surrounding the target sites amplified from these sorted cells. Fifty clones were randomly picked up for direct DNA sequencing. Thirty-eight of these clones showed various deletions at the cleavage site (**Figure 4b** and **4c**, and see **Supplementary Figure S4a** online), suggesting that our TALEN pair induced approximately 76% gene modification in the target site. Since NIH 3T3 cells are diploid,[39] we estimated that more than 52% of the cells had MSTN gene disruption on both alleles (see **Supplementary Figure S4b** online). Among the 38 mutant clones, 24 had frame-shift deletions or insertions, and the other 14 had in-frame deletions or mis-sense point mutations. These statistics are consistent with the randomness of NHEJ DNA repair.

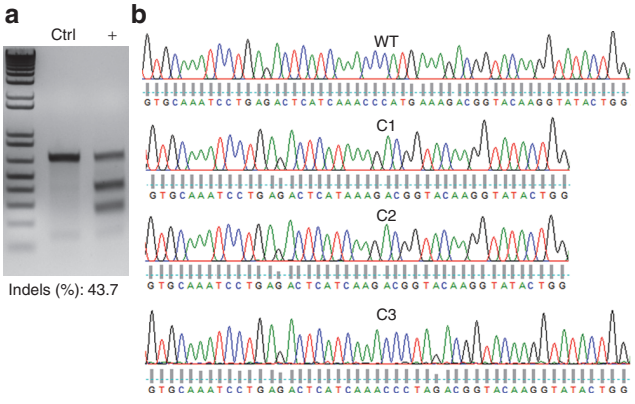

c

	Left binding site	Cleavage site	Right binding site
WT:	GTGCAAATCCTGAGACT	CATCAAACCCATGAAAG	ACGGTACAAGGTATACTGG
C1:	GTGCAAATCCTGAGACT	CAT----------AAAG	ACGGTACAAGGTATACTGG
C2:	GTGCAAATCCTGAGACT	CATC----------AAG	ACGGTACAAGGTATACTGG
C3:	GTGCAAATCCTGAGACT	CATCAAACCC-T---AG	ACGGTACAAGGTATACTGG
C4/5:	GTGCAAATCCTGAGACT	CATCAA-----TGAAAG	ACGGTACAAGGTATACTGG
C6:	GTGCAAATCCTGAGACT	CATCAAACC---GAAAG	ACGGTACAAGGTATACTGG
C7:	GTGCAAATCCTGAGACT	CATC---------AAAG	ACGGTACAAGGTATACTGG
C8:	GTGCAAATCCTGAGACT	CAT------CATGAAAG	ACGGTACAAGGTATACTGG

Figure 4 Sequence analysis of the MSTN locus after MSTN TALENs-mediated gene editing. (**a**) Gene-editing efficiency was measured using T7E1 assay in sorted NIH 3T3 cells transfected with the EGFP-tagged MSTN TALENs-encoding plasmid. (**b**) Sequencing analysis of the *MSTN* allele in the sorted NIH 3T3 cells. DNA fragments surrounding the TALEN target sites were PCR amplified from the sorted NIH 3T3 cells and cloned into a vector backbone. Fifty clones were randomly picked up for direct DNA sequencing. Sequencing data of four clones (C1, C2, C3 and WT [C9]) were shown in panel B. (**c**) Sequence variations of first eight clones at the cleavage site were aligned with WT sequence (the sequences of the other clones were listed in **Supplementary Figure S4a** online). As compared with the WT DNA, eight clones had various deletions in the cleavage site. Clones C4 and C5 carry the same deletions.

High sequence specificity of the MSTN TALENs

In our TALEN engineering, the RVD Asn-Asn (NN), which recognizes both guanine and adenine,[29] was used for guanine. One potential problem with the dual recognition by NN is an increase of off-target activity. We searched the potential off-target sites by running the RVDs in the "Paired Target Finder" tool maintained by TAL Effector Nucleotide Targeter 2.0 (https://tale-nt.cac.cornell.edu/node/add/talef-off-paired).[27,30] TALEN-mediated DNA cleavage can occur wherever two TALEN monomers bind with the proper spacing and orientation. Thus, a search for off-target sites must consider all four possible combinations of TALEN monomer RVD sequences: RVD1+RVD1, RVD1+RVD2, RVD2+RVD1, and RVD2+RVD2. But since our TALEN pair used obligate heterodimer variants of the FokI cleavage, the RVD1+RVD1 or RVD2+RVD2 combinations would form a less active dimer (in the case of ELD variant) or nonfunctional dimer.[34] We thus only consider RVD1+RVD2 or RVD2+RVD1 combinations. In total, ten potential off-target sites with these two combinations can be identified in the human genome (see **Supplementary Table S2** online). Manual examination of these sites revealed that at least four different nucleotides within each half site are not recognized by RVDs specifically targeting human MSTN target site, even if the dual recognition of NN was taken into consideration. To directly examine the off-target activity of our MSTN TALENs, we selected top three potential target sites located on three different chromosomes as listed in see **Supplementary Table S2** online and used the T7E1 assay for each of these sites. As shown in **Figure 5**, no detectable gene editing activities were observed in any of these sites. These data suggest that the TALENs-mediated gene editing is highly sequence specific.

TALEN-mediated gene editing in primary mouse and human myoblasts

Next, we tested the efficiency of gene editing in primary mouse and human myoblasts using our MSTN TALEN pair. We established a myoblast culture from *flexor digitorum brevis* (FDB) muscle of a dysferlin-deficient mouse model.[39] Primary human myoblasts from control and dysferlinopathy patients were obtained from Telethon Network of Genetic Biobanks. These primary myoblasts exhibited low transfection efficiency with regular lipid or nonlipid transfection reagents. To overcome this challenge, we utilized the Neon Transfection System (Invitrogen, Carlsbad, CA). The T7E1 assay confirmed that MSTN TALENs induced high frequency (10.3% to 24.6%) of gene editing in all these primary myoblast cultures (**Figure 6**).

TALENs-mediated functional disruption of the *MSTN* gene

To examine the functional outcomes of MSTN TALENs-induced gene disruption in muscle cells, we screened six individual clones of C2C12 cells that were sorted for positive transfection of MSTN TALENs. The genomic DNA of all six clones were further analyzed by DNA sequencing. Five of these clones carried biallelic myostatin gene disruption at the TALEN cleavage site (**Figure 7a**) while clone #2 was WT. Several mutations were in-frame deletion or point mutation. We selected clones #1, 2, and 3 for further analysis. The

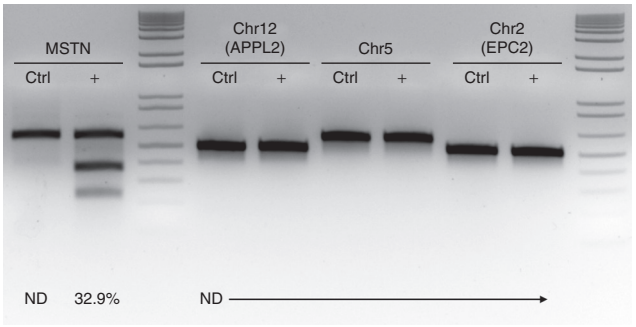

Figure 5 Off-target activities of the MSTN TALENs. No detectable gene-editing activities by the MSTN TALENs were observed at three top potential off-target sites located on three different chromosomes in HEK293 cells as examined by T7E1 assay. ND, not detected.

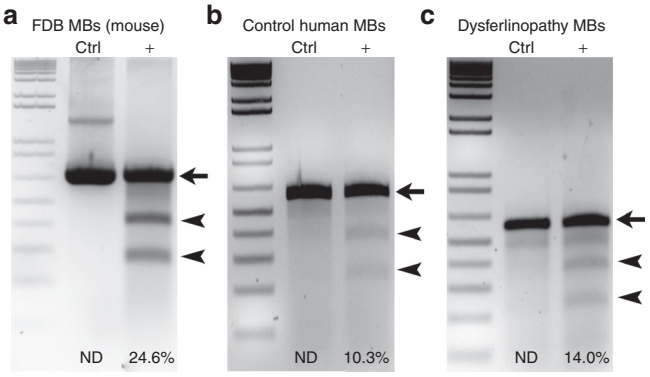

Figure 6 MSTN TALENs-mediated gene editing in primary human and mouse myoblasts. Gene-editing activity were observed in three lines of primary myoblasts: (**a**) Mouse myoblasts derived from FDB muscles, (**b**) Human control myoblasts and (**c**) dysferlinopathy patient myoblasts after electroporation-mediated transfection of MSTN TALENs. ND, not detected.

cells of these three clones were induced to differentiate for 3 days by replacing the growth media with the differentiation media. Dexamethasone was added into the media on day 3 and cultured for another three days. Dexamethasone is a glucocorticoid known to induce myostatin expression and atrophy in C2C12 myotubes.[40] Indeed, the WT clone #2 showed dexamethasone-induced atrophy while the other two *MSTN*-mutant clones continued to grow larger even in the presence of dexamethasone (**Figure 7b** and **7c**). Western blotting analysis demonstrated that myostatin expression was disrupted in both clone #1 and 3 as compared with the control cells or clone #2 (**Figure 7d**). These data suggest that the expression of myostatin is involved in dexamethasone-induced myotube atrophy.

TALENs-mediated integration of transgenes into the *MSTN* locus

Double-strand breaks can be repaired by homologous recombination (HR). Thus, ZFNs and TALENs are valuable tools to introduce targeted gene addition to the specific genomic locus. To promote gene insertion at the target site, a donor plasmid was constructed that contains two homology arms (800 base pairs) which surround the human *MSTN* target site separated by a complete expression cassette for

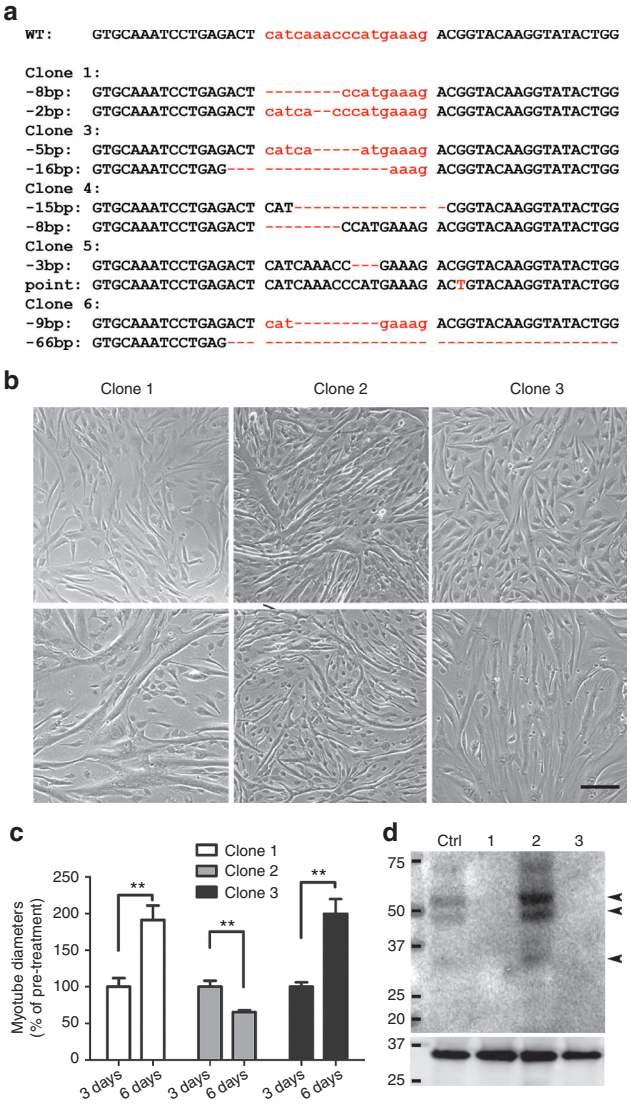

Figure 7 Disrupted myostatin protein expression in C2C12 cells after treatment with MSTN TALENs. (**a**) Genomic DNA sequencing results of individual C2C12 clones. (**b**) Bright field micrographs of C2C12 myotubes from the three clones on Day 3 and Day 6. The cells were treated with 100 nmol/l dexamethasone (Dex) on Day 3 to 6. Scale bar: 100 μm. (**c**) Quantitative measurement of myotube diameters. Results are mean ± SEM. $^{**}P < 0.01$. (**d**) Western blotting analysis of myostatin expression in three individual C2C12 clones after treatment with MSTN TALENs. Arrows indicate the myostatin bands ~52, 43 and 28 kDa, respectively. GAPDH was used as a loading control.

mCherry-puromycin driven by a CMV promoter (**Figure 8a**). Cotransfection of MSTN TALENs and donor plasmid into HEK293 cells (initial cell number: 5×10^5 cells) allows formation of mCherry-positive colonies after puromycin selection (**Figure 8b**). Specific integration of the expression cassette was identified by PCR with primers (see supplementary **Materials and Methods** for details) that bind inside mCherry and inside the MSTN genomic DNA beyond the left homology arm. Only specific integration events generate a PCR product. No targeted integration events were detected in cell pool that was transfected with the donor plasmid alone (**Figure 8c**). However, when MSTN TALENs were cotransfected with the donor plasmid together, mCherry-puromycin cassette was efficiently integrated into the *MSTN* locus at the target site (**Figure 8c**). Similarly, we constructed a mouse version of the donor plasmid and tested TALENs-mediated integration of mCherry-puromycin cassette in mouse C2C12 cells. Again, specific integration of the expression cassette was only detected in C2C12 cells cotransfected with MSTN TALENs and the donor plasmid, but not in cells transfected with the donor only (see **Supplementary Figure S5** online).

Next, we examined the feasibility of targeted integration of a larger gene cassette into the human *MSTN* locus facilitated by TALENs. For this purpose, we constructed a donor vector that carries a mCherry-puromycin and enhanced cyan fluorescent protein (ECFP)-tagged dysferlin, a gene mutated in limb-girdle muscular dystrophy type 2B and Miyoshi myopathy patients, linked by a self-cleaving 2A peptide sequence (**Figure 9a**). The entire expression cassette flanked by the left and right homology arms is ~9.3kb in length. Codelivery of both MSTN TALENs and the donor vector resulted in the formation of colonies showing both mCherry and ECFP fluorescence after puromycin selection (initial cell number: 5×10^5) (**Figure 9b**). Previous studies showed that dysferlin is primarily localized at the plasma membrane due to the presence of a single transmembrane domain in the very C-terminus. Indeed, the ECFP fluorescence showed a typical plasma membrane pattern (see **Supplementary Figure S6** online) suggesting the full-length dysferlin was expressed. PCR genotyping confirmed the targeted integration in pooled cells cotransfected with TALENs and donor while no targeted integration occurred in donor only cells (see **Supplementary Figure S7** online). We also picked up four individual colonies from each transfection group and performed PCR genotyping analysis. Two colonies that were positive for CFP-dysferlin in the cotransfected cells showed the correct PCR product indicating targeted integration (**Figure 9c**), and all colonies in the donor only group had no predicted PCR product even though they mostly have dysferlin indicating only random integration in these cells (**Figure 9c**).

Discussion

Gene modified cells and animals are widely employed in basic biomedical research and biotechnological applications. This is often achieved by random gene integration into the genome either by retroviral transduction, or plasmid transfection and selection for stable clones. These strategies can be labor and cost intensive, requiring clone screening to identify clones with a suitable expression level. ZFNs and TALENs are two new classes of engineered enzymes for targeted genome editing in various cell types. In this study, we successfully applied the TALEN technology to modify *MSTN* loci in multiple mammalian cells using a single highly efficient TALEN pair.

Our MSTN-TALEN pair was engineered based upon GoldyTALEN scaffold which allows greater cleavage and genetic modification efficiency in comparison with others.[27,41] Indeed, this TALEN pair induced approximately 10–30% mutation

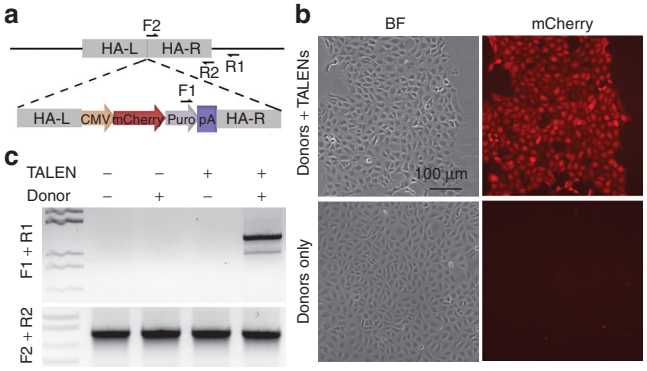

Figure 8 MSTN TALENs facilitate targeted addition of a marker gene into the human *MSTN* locus. (**a**) A schematic showing homologous recombination between genomic DNA and the donor DNA carrying a mCherry-puromycin cassette flanked by the left and right homology arms (HA-L and HA-R). The arrows indicate the relative positions of primers used for genotyping analysis. (**b**) Cotransfection of the donor plasmid and the plasmid encoding MSTN TALENs into HEK293 cells resulted in the formation of many mCherry-positive clones after puromycin selection for a week. Some clones formed in the cells transfected with only donor plasmid do not show mCherry fluorescence, indicating random integration events. Scale bar = 100 μm. (**c**) Genotyping analysis of the bulk transfected HEK293 cells with no plasmid, donor only, TALENs only, or donor plus TALENs, using the primers F1 and R1 or F2 and R2. The cells were collected 48 hours after transfection.

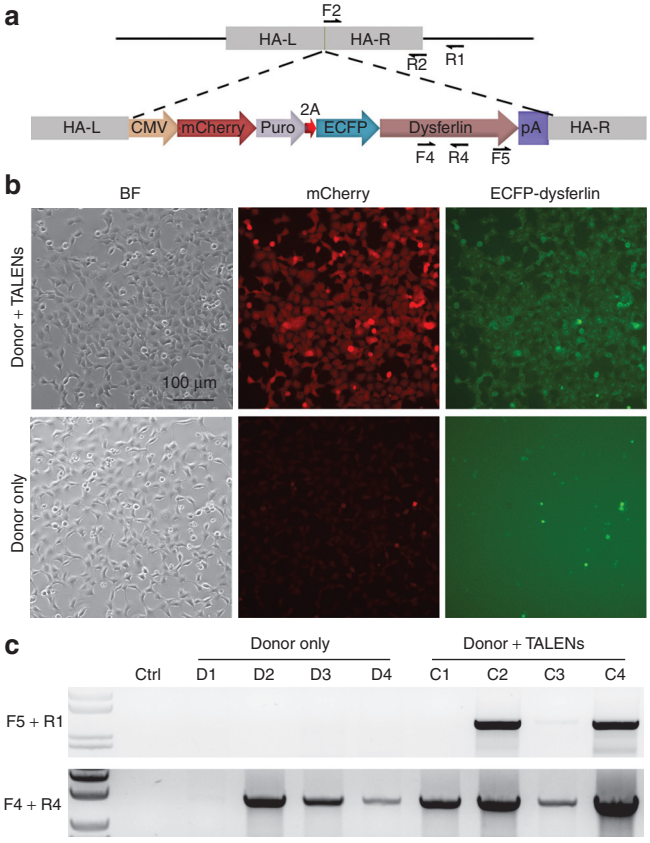

Figure 9 MSTN TALENs facilitate targeted integration of a dysferlin expression cassette into the human *MSTN* locus. (**a**) A schematic showing homologous recombination between genomic DNA and the donor DNA carrying a mCherry-puromycin-2A-ECFP-dysferlin cassette flanked by the left and right homologous arms (HA-L and HA-R). (**b**) Cotransfection of the donor plasmid and the plasmid encoding MSTN TALENs into HEK293 cells resulted in the formation of many mCherry and ECFP-positive clones after puromycin selection for a week. Most clones formed in the cells transfected with only donor plasmid do not show both mCherry and ECFP fluorescence, indicating random integration events. Scale bar = 100 μm. (**c**) Genotyping analysis of individual colonies isolated from the HEK293 cells transfected with either donor only or donor plus TALENs using the primer combinations as follows: F5 and R1, F4 and R4, or F2 and R2. Nontransfected cells were used as control (Ctrl).

frequency in various cell lines and primary myoblast cultures examined, as measured by T7E1 assay on a regular TAE agarose gel. The mutation rates as determined are obviously underestimated because the *in vitro* transfection efficiency can never reach 100%. To calculate the gene editing efficiency more accurately, we fused an EGFP tag with the TALENs and the transfected cells were sorted by FACS for EGFP. When only EGFP-positive cells were analyzed for mutation rates induced by the TALENs, the estimated mutation frequency is increased to around 45%. We believe this number is still underestimated due to the fact that additional factors, such as formation of homoduplex during reannealing process and limited sensitivity of gel densitometry, can influence the calculation using the T7E1 assay. As an alternative approach, we randomly sequenced 50 clones of the TALEN-target region and found that 38 of these clones carried small deletions/insertions/point mutations. This suggests that our TALEN pair produced about 76% gene editing frequency, consistent with previous reports that high genome editing efficiency can be achieved using the GoldyTALEN scaffold.[27,41] Based on this, we estimate that at least 52% of the cells have double allele mutation (see **Supplementary Figure S4** online). This estimation is further supported by experimental data in C2C12 cells, for which we randomly picked up six clones and identified five of them carry double allele mutations (**Figure 7a**). Our data suggest that it is feasible to generate double allele knockout cells without drug selection using the TALEN approach.

Our TALEN pair precisely targets Exon 2 of human *MSTN* locus. Exon 2 is a naturally occurring mutation site in certain species of cattle with extra-developed muscles.[3] Most of the mutations induced by these TALENs are small deletions, disrupting the reading frame (**Figures 4** and **7c**) and predicted to completely knock out the expression of myostatin. Indeed, western blotting and functional analyses demonstrated that TALEN-mediated MSTN gene disruption led to dramatic reduction in the expression of myostatin (**Figure 7b** and **7c**). Interestingly, even in-frame deletions still disrupted the myostatin expression (data not shown). These data suggest that targeting exon 2 is a viable approach to disable the function of myostatin. Our data also suggest that myostatin-induced atrophy is, at least in part, through the expression of myostatin. Thus, the TALEN-mediated gene disruption approach can allow rapid gene function analysis in cell culture.

The target sites of our TALEN pair are highly conserved in mammals (see **Supplementary Figure S3** online). In particular, these sequences are exactly the same in primates and farm animals such as pig, cattle and horse. Thus, our MSTN TALENs are predicted to work in all primates and many other

mammals. Rapid generation of *MSTN* knockout cells and animals from these species could be achieved using this single pair of TALENs. Already, TALEN-induced knockout and knockin farm animals have been developed in pigs and cows with high efficiency.[42,43]

The MSTN TALENs seem to be highly specific. In the human genome, there are only 10 similar sequences to the target site (see **Supplementary Table S2** online), and we did not detect any off-target activity at three most similar target sites using the T7E1 assay (**Figure 5**). These data suggest that these TALENs are highly sequence specific. However, it is worth noting that there are limitations in detecting genome-editing activities using the T7E1 assay. For example, it is not possible to detect rare genome editing events using this assay.

The ability of TALENs to stimulate HR by creating double-strand break is of interest in context of targeted gene addition in cell engineering for cell therapy or other purposes. Our data suggest that a large DNA sequence of at least 9.3kb can be efficiently integrated via HR into the human *MSTN* locus. In particular, targeted addition of a therapeutic gene such as dysferlin, which is defective in a group of muscular dystrophy patients, into the *MSTN* locus of myoblasts would offer significant benefit for a myoblast-based therapy approach. *MSTN* is typically expressed in developing and adult skeletal muscle;[1] addition of the therapeutic genes for muscular dystrophies into the *MSTN* locus would allow persistent expression of such genes in skeletal muscle. Our experiment carried out on a human cell line demonstrated that a dysferlin expression cassette can be efficiently integrated into the human *MSTN* locus, allowing persistent and uniform expression of dysferlin. It would be interesting to see whether this MSTN TALEN pair can facilitate gene addition into primary human and mouse myoblasts, which can be used for myoblast transplantation therapy in the future.

In summary, TALEN is an effective genome-editing tool. Application of MSTN TALENs in a variety of cell lines and species would allow further investigation of myostatin functions in mammalian animals that do not have naturally occurring mutant *MSTN* models yet. Moreover, this TALEN pair would also be a valuable tool for cell engineering in translational research such as myoblast transplantation therapy to replace defective genes in genetic diseases including muscular dystrophy.

Materials and methods

Assembly of MSTN-TALENs. We constructed a pair of TALENs to target the MSTN locus using the published Golden Gate platform.[27] The Golden Gate TALEN kit (Kit#1000000016) was obtained from Addgene. TALENs were assembled in the same way as described[27] with the following modifications. Instead of the pTAL scaffold,[27] we used the GoldyTALEN scaffold[41] to construct our TALENs because GoldyTALEN scaffold has an increased gene-editing efficiency. The GoldyTALEN scaffold was constructed by PCR using the following primer pairs: TAL-F1, CAAGGTACCTATGGT GGATCTACGCACGCTCGGCTACAG; TAL-R1, ACGGTCGA CGTCTCCAGGGGAGCACCCGTCAGTGCATTG; TAL-F2, GACGTCGACCGTCTCCAACGACCACCTCGTC; TAL-R2, TTGGGATCCGGCAACGCGATGGGACGTGCGTTC. The two PCR fragments were ligated into the KpnI and BamHI sites of a mammalian expression plasmid designated as pTAL5, which is based upon pEGFP-C3 with the following modifications: (i) a 3xFLAG tag and nucleus localization signal (NLS) sequence, (ii) a wild-type (WT) FokI domain, and (iii) BsaI and BsmBI sites removed outside of the GoldyTALEN scaffold. The final pTAL5 plasmid contains a unique BsmBI site within the scaffold in order to be compatible with the Golden Gate platform. To construct TALENs with obligate heterodimer variants of the FokI domain (ELD-sharkey and KKR-sharkey), we used QuikChange II Site-Directed Mutagenesis kit (Agilent Technologies, Cedar Creek, TX) to obtain the ELD-sharkey and KKR-sharkey variants. To streamline the assembly of a functional pair of TALENs into one plasmid, we placed two GoldyTALEN scaffolds linked by a self-cleaving 2A peptide into a final plasmid designated as pTAL6, which has a unique BsaI site instead of BsmBI site within the second GoldyTALEN scaffold. Both pTAL5 and pTAL6 are available upon request. The protein sequences of MSTN TALENs are provided in the **Supplementary Figures S1 and S2** online).

Construction of mouse and human donor plasmids. The homology arms (~800 bp) of the human and mouse *MSTN* locus were PCR amplified from genomic DNA of mouse C2C12s cell or human HEK293 cells. The primer sequences are as follows: hGDF8-HL-F: 5′-ATC TACTAGTGCCTGGCCCTAAAGACAAT-3′; hGDF8-HL-R: 5′-ATCTGGTACCTCTAGATTGTAGGAGTCTCGACGGG-3′; hGDF8-HR-F:5′-TCTGGTACCGATATCCTCTGAAACTTGAC ATGAACCC-3′; hGDF8-HR-R: 5′-ATCTGCGGCCGCCCAC ATCAGTGCATCAACATCC-3′; mGDF8-HL-L: CGTACTAGT CAAGGCCACTGCTTTCTGAT-3′; mGDF8-HL-R: AGACTCG AGAAACACTGTTGTAGGAGTCTTGAC-3′; mGDF8-HR-L: A GCCTCGAGAGCGATATCCGATCTCTGAAACTTGAC-3′; mGDF8-HR-R: ATCTGCGGCCGCGCAAGTATGCTAAAGGA GTCCA-3′. PCR products for left and right arms were digested with SpeI/KpnI and KpnI/NotI, respectively and ligated into SpeI and NotI restriction sites of AAVS1 SA-2A-puro-pA donor plasmid (#22075 from Addgene) to generate human and mouse GDF8 donor plasmids. To add a mCherry-puromycin expression cassette with a CMV promoter, we assembled the following pieces together: (i) a CMV promoter was amplified from pmCherry-C1 plasmid (Clontech, Mountain View, CA) with primers: CMV-F, AGTGGTCTCCACCGTCGACTAGTTAT TAATAGTAATCAATTACGGGGTC-3′ and CMV-R, ACTCTC GAGAGCGCTAGCGGATCTGACGGTTCACTAAAC-3′ and the PCR product was digested with SpeI and NheI; (ii) mCherry fragment was obtained by digesting pmCherry-C1 plasmid (Clontech, Mountain View, CA) with Nhe1 and Sal1; and (iii) puromyocin was obtained from AAVS1 SA-2A-puro-pA donor plasmid (#22075 from Addgene) by XhoI and NotI. These three fragments were ligated into the SpeI and NotI site of the human or mouse GDF8 donor plasmids to create the final human or mouse GDF8 donor plasmids carrying a complete mCherry-puromycin expression cassette. Moreover, a ECFP-dysferlin fragment fused to mCherry-puromycin with a 2A self-cleaving peptide sequence was added to form the mCherry-puromycin-2A-ECFP-dysferlin donor plasmids.

Cell culture and transfection. HEK293, BAEC, NIH 3T3, HT1080, and C2C12 cells were cultured in DMEM supplemented with 10% FBS. Cells were seeded in six-well plates until they reached ~80% confluence. HEK293 cells were transfected with 2 µg TALENs-encoding plasmid using X-tremeGENE HP DNA transfection reagent (Roche, Indianapolis, IN) and media was changed after 24 hours. Typically, this resulted in about 60% transfection efficiency. BAEC, NIH3T3, HT1080, and C2C12 cells were transfected with 7.5 µg TALENs-encoding plasmid with Xfect transfection reagent (Clontech, Mountain View, CA) and media was changed after 4 hours. The cells were assayed 48 hours after transfection. The transfection efficiency for BAEC varies from 20 to 30%, and for NIH 3T3, C2C12 and HT1080 cells varies from 10 to 20% (we thus did three rounds of transfection). Primary mouse and human myoblasts (#10067 control patient and #9501 dysferlin-deficient patient, obtained from Telethon Genetic BioBank Network) were cultured in DMEM/F-12 supplemented with 20% FBS. These primary myoblasts were transfected with Neon Transfection System (Invitrogen, Carlsbad, CA). Briefly, 1×10^5 cells were electroporated with 0.5 µg TALENs-encoding plasmid. The electroporation conditions for mouse FDB myoblasts and human myoblasts were 1700 V, 20 ms, 1 pulse and 1400 V, 20 ms, 2 pulses, respectively. These conditions consistently resulted in about 50% transfection efficiency in mouse FDB myoblasts with about 20% survival rate and 30% transfection efficiency in human myoblasts with 20% survival rate.

T7E1 mismatch-detecting assay. The cleavage activities of the MSTN TALENs were assayed by mismatch-recognizing T7E1 as described previously.[31] The T7E1 assay detects small deletion/insertion mutations (indels) originated from NHEJ DNA repair events following TALENs-induced double-strand break. Briefly, the cells transfected with TALENs-expressing plasmid were harvested 3 days post-transfection and genomic DNA was extracted. A DNA fragment surrounding the TALEN target site was amplified by PCR with the AccuPrime PCR kit (Invitrogen, Carlsbad, CA). The primer pairs were 5′-TGGAGGGGTTTTGTTAA TGG-3′ and 5′-TATTGGGTACAGGGCTACCG-3′ for human, 5′-AGTGGTCTCACTATACGTACACACTACCCCAACAGC-3′ and 5′- AGTGGTCTCACGCCCATGGGACATGAGATTGACA CA-3′ for mouse, and 5′-TCC CGAGGCTCAGTTAGTTGC-3′ and 5′-CACTGGGGTAAGGCACCTTTG-3′ for bovine. The primer pairs used to detect off-target activities were 5′- TCTT ATCTGCTGGGCCACTC-3′ and 5′- CTGCTCCCGTTTTCTG TAGC-3′ for human chromosome 5 site, 5′- CACAGGACATG TGGGAACAG-3′ and 5′- GCCCAATGGAAAATCGTATG-3′ for human chromosome 12 site, 5′- GTTGTGGGACC AAAGACGAT-3′ and 5′- ACGCTGGGAATTTCCTCTCT-3′ for human chromosome 2 site. The DNA fragment was purified and denatured at 95 °C for 10 minutes, and reannealed slowly using the following temperature program: 90 cycles of 95 to 59 °C with a 0.4 °C decrease per cycle for 20 seconds, 90 cycles of 59 to 32 °C with a 0.3 °C decrease per cycle for 20 seconds, 20 cycles of 32 to 26 °C with a 0.3 °C decrease per cycle for 20 seconds. This allows the formation of DNA heteroduplex if NHEJ occurred. The reannealed DNA samples were incubated with 0.5 µl T7E1 (New England BioLabs, UK) for 45 minutes and subjected to electrophoresis on a 2% TAE agarose gel. The gels were stained with ethidium bromide and imaged using Chemidoc (BioRad, Hercules, CA). Densiometric quantification of DNA bands was done using ImageJ. Mutation frequencies were calculated using the formula: fractional modification = 1– (1– (fraction cleaved))$^{0.5}$ as described.[32]

Fluorescence-activated cell sorting (FACS). Two days after transfection with EGFP-tagged MSTN-TALEN plasmid, NIH 3T3 cells and C2C12 cells were sorted by FACS (FACSAria II, BD) to enrich EGFP-positive cells. The sorted EGFP-positive cells were further cultured for 1 week and then the genomic DNA was extracted. The genomic DNA of sorted cells was analyzed for gene-editing activities by T7E1 assay. DNA fragment surrounding the TALEN target sites were PCR amplified from the genomic DNA of sorted cells with a forward primer 5′-AGTGGTCTCACTATACGTACACACTACCCCAACAGC-3′ and a reverse primer 5′-AGTGGTCTCACGCCCATGGGA CATGAGATTGACACA-3′. The PCR products were digested with SnaBI and NcoI restriction enzymes, and subcloned into a temporary vector based on pFastBac (Invitrogen, Carlsbad, CA). Ten clones were randomly picked up for direct DNA sequencing.

PCR genotyping of targeted integration. HEK293 cells in six well plates were transfected with 1 µg MSTN-TALEN and 1 µg human donor plasmid using X-tremeGENE HP DNA transfection Reagent (Roche, Indianapolis, IN). C2C12 cells were transfected with 4 µg MSTN-TALEN and 6 µg mouse donor plasmid using Xfect reagent (Clontech). After 48 hours, genomic DNA was extracted and targeted integration events in cell lines were identified by PCR analysis. The primers used are provided in **Supplementary Table S1** online.

Fluorescence microscopy. Fluorescence and bright-field images were taken with NIS-Elements Advanced Research software package (Nikon, Tokyo, Japan) using an inverted Nikon Ti-E microscope equipped with a Xenon lamp (Hamamatsu Photonics Systems, Bridgewater, NJ), a 40x 1.30 NA objective (Nikon, Tokyo, Japan), and an Evolve 512 EMCCD camera (Photometrics, Pleasanton, CA). The EMCCD camera was cooled to –80 °C during imaging. ECFP-dysferlin integrated cells were also imaged with a confocal microscope (TCS-SP5, Leica Microsystems, Wetzlar, Germany), using the 514 nm line of an argon continuous laser as the excitation source. Fluorescence emission was collected with a 63x water immersion objective (HCX PL APO, 1.2 NA).

Western blotting. Cells were lysed with cold RIPA buffer supplemented with protease inhibitors and extracted protein samples were separated by SDS-PAGE and transferred onto Nitrocellulose membranes (0.45 µm). The mouse monoclonal anti-FLAG (Sigma-Aldrich, Saint Louis, MO), rabbit polyclonal anti-myostatin (#ab98337, Abcam), and rabbit monoclonal anti-GAPDH (Cell Signaling) antibodies were used for immunoblotting analysis. HRP conjugated rabbit antimouse and goat antirabbit secondary antibodies were obtained from Millipore, Billerica, MA. The membranes were developed using ECL2 western blotting substrate (Pierce Biotechnology, Rockford, IL) and imaged using ChemiDoc XRS+ system with Image Lab software (Bio-Rad).

Measurement of myotube diameter. Myotube cultures were photographed with a Nikon Ti-E microscope (as mentioned above) after 3 days and 6 days differentiation. Dexamethesone (100 μM) was added into the cultures on day 3 to day 6. The diameters were measured as previously described.[44] Briefly, a total of 35–62 myotubes in different groups from at least five random fields were measured using ImageJ software (NIH, Frederick, MD). The measurements were conducted in a "blinded" fashion on coded pictures with the investigator being unaware of the group from which the cultures originated. Results were expressed as per cent of the diameters on day 3.

Supplementary material

Table S1. Primers used for genotyping analysis of HR integration.
Table S2. List of potential off-target sites of the MSTN TALEN pair.
Figure S1. Amino acid sequences of the left MSTN TALEN.
Figure S2. Amino acid sequences of the right MSTN TALEN.
Figure S3. Sequence alignment of the MSTN genes from various species at the TALEN target sites.
Figure S4. Sequence variants in additional clones (**a**) and estimation of biallelic genome-editing activities (**b**).
Figure S5. Genotyping analysis of C2C12 cells transfected with either donor (mCherry-puromycinR) only, TALENs only, or donor plus TALENs.
Figure S6. Confocal images of HEK293 cells integrated with mCherry-puromycinR-2A-ECFP-dysferlin donor.
Figure S7. Genotyping analysis of HEK293 cells transfected with either donor (mCherry-puromycinR-2A-ECFP-dysferlin) only, TALENs only, or donor plus TALENs.

Acknowledgments. We thank Marina Mora (Telethon Genetic BioBank Network) for providing primary human myoblasts (#10067 and #9501), Jody Martin (Loyola University Chicago) for HT1080 cells, Ajay Rana (Loyola University Chciago) for NIH 3T3 cells and Matthias Majetschak (Loyola University Chicago) for BAEC cells. This work was partially supported by the American Heart Association (10SDG4140138 to R.H.) and the Muscular Dystrophy Association (MDA171667 to R.H.). We declare that no conflict of interest exists.

1. McPherron, AC, Lawler, AM and Lee, SJ (1997). Regulation of skeletal muscle mass in mice by a new TGF-beta superfamily member. *Nature* **387**: 83–90.
2. Schuelke, M, Wagner, KR, Stolz, LE, Hübner, C, Riebel, T, Kömen, W *et al.* (2004). Myostatin mutation associated with gross muscle hypertrophy in a child. *N Engl J Med* **350**: 2682–2688.
3. Grobet, L, Martin, LJ, Poncelet, D, Pirottin, D, Brouwers, B, Riquet, J *et al.* (1997). A deletion in the bovine myostatin gene causes the double-muscled phenotype in cattle. *Nat Genet* **17**: 71–74.
4. Kambadur, R, Sharma, M, Smith, TP and Bass, JJ (1997). Mutations in myostatin (GDF8) in double-muscled Belgian Blue and Piedmontese cattle. *Genome Res* **7**: 910–916.
5. McPherron, AC and Lee, SJ (1997). Double muscling in cattle due to mutations in the myostatin gene. *Proc Natl Acad Sci USA* **94**: 12457–12461.
6. Clop, A, Marcq, F, Takeda, H, Pirottin, D, Tordoir, X, Bibé, B *et al.* (2006). A mutation creating a potential illegitimate microRNA target site in the myostatin gene affects muscularity in sheep. *Nat Genet* **38**: 813–818.
7. Mosher, DS, Quignon, P, Bustamante, CD, Sutter, NB, Mellersh, CS, Parker, HG *et al.* (2007). A mutation in the myostatin gene increases muscle mass and enhances racing performance in heterozygote dogs. *PLoS Genet* **3**: e79.
8. Sakuma, K and Yamaguchi, A (2010). Molecular mechanisms in aging and current strategies to counteract sarcopenia. *Curr Aging Sci* **3**: 90–101.
9. Bogdanovich, S, Krag, TO, Barton, ER, Morris, LD, Whittemore, LA, Ahima, RS *et al.* (2002). Functional improvement of dystrophic muscle by myostatin blockade. *Nature* **420**: 418–421.
10. Roth, SM and Walsh, S (2004). Myostatin: a therapeutic target for skeletal muscle wasting. *Curr Opin Clin Nutr Metab Care* **7**: 259–263.
11. Bishop, A, Kambadur, R and Sharma, M (2005). The therapeutic potential of agents that inactivate myostatin. *Expert Opin Investig Drugs* **14**: 1099–1106.
12. Lee, SJ and Glass, DJ (2011). Treating cancer cachexia to treat cancer. *Skelet Muscle* **1**: 2.
13. Murphy, KT, Cobani, V, Ryall, JG, Ibebunjo, C and Lynch, GS (2011). Acute antibody-directed myostatin inhibition attenuates disuse muscle atrophy and weakness in mice. *J Appl Physiol* **110**: 1065–1072.
14. Nakatani, M, Takehara, Y, Sugino, H, Matsumoto, M, Hashimoto, O, Hasegawa, Y *et al.* (2008). Transgenic expression of a myostatin inhibitor derived from follistatin increases skeletal muscle mass and ameliorates dystrophic pathology in mdx mice. *FASEB J* **22**: 477–487.
15. Parsons, SA, Millay, DP, Sargent, MA, McNally, EM and Molkentin, JD (2006). Age-dependent effect of myostatin blockade on disease severity in a murine model of limb-girdle muscular dystrophy. *Am J Pathol* **168**: 1975–1985.
16. Whittemore, LA, Song, K, Li, X, Aghajanian, J, Davies, M, Girgenrath, S *et al.* (2003). Inhibition of myostatin in adult mice increases skeletal muscle mass and strength. *Biochem Biophys Res Commun* **300**: 965–971.
17. Porteus, MH and Carroll, D (2005). Gene targeting using zinc finger nucleases. *Nat Biotechnol* **23**: 967–973.
18. Smith, J, Bibikova, M, Whitby, FG, Reddy, AR, Chandrasegaran, S and Carroll, D (2000). Requirements for double-strand cleavage by chimeric restriction enzymes with zinc finger DNA-recognition domains. *Nucleic Acids Res* **28**: 3361–3369.
19. Moehle, EA, Moehle, EA, Rock, JM, Rock, JM, Lee, YL, Lee, YL *et al.* (2007). Targeted gene addition into a specified location in the human genome using designed zinc finger nucleases. *Proc Natl Acad Sci USA* **104**: 3055–3060.
20. Kim, YG, Cha, J and Chandrasegaran, S (1996). Hybrid restriction enzymes: zinc finger fusions to Fok I cleavage domain. *Proc Natl Acad Sci USA* **93**: 1156–1160.
21. Smith, J, Berg, JM and Chandrasegaran, S (1999). A detailed study of the substrate specificity of a chimeric restriction enzyme. *Nucleic Acids Res* **27**: 674–681.
22. Li, H, Haurigot, V, Doyon, Y, Li, T, Wong, SY, Bhagwat, AS *et al.* (2011). *In vivo* genome editing restores haemostasis in a mouse model of haemophilia. *Nature* **475**: 217–221.
23. Perez, EE, Wang, J, Miller, JC, Jouvenot, Y, Kim, KA, Liu, O *et al.* (2008). Establishment of HIV-1 resistance in CD4+ T cells by genome editing using zinc-finger nucleases. *Nat Biotechnol* **26**: 808–816.
24. Mussolino, C, Morbitzer, R, Lütge, F, Dannemann, N, Lahaye, T and Cathomen, T (2011). A novel TALE nuclease scaffold enables high genome editing activity in combination with low toxicity. *Nucleic Acids Res* **39**: 9283–9293.
25. Li, T, Huang, S, Zhao, X, Wright, DA, Carpenter, S, Spalding, MH *et al.* (2011). Modularly assembled designer TAL effector nucleases for targeted gene knockout and gene replacement in eukaryotes. *Nucleic Acids Res* **39**: 6315–6325.
26. Hockemeyer, D, Wang, H, Kiani, S, Lai, CS, Gao, Q, Cassady, JP *et al.* (2011). Genetic engineering of human pluripotent cells using TALE nucleases. *Nat Biotechnol* **29**: 731–734.
27. Cermak, T, Doyle, EL, Christian, M, Wang, L, Zhang, Y, Schmidt, C *et al.* (2011). Efficient design and assembly of custom TALEN and other TAL effector-based constructs for DNA targeting. *Nucleic Acids Res* **39**: e82.
28. Moscou, MJ and Bogdanove, AJ (2009). A simple cipher governs DNA recognition by TAL effectors. *Science* **326**: 1501.
29. Boch, J, Scholze, H, Schornack, S, Landgraf, A, Hahn, S, Kay, S *et al.* (2009). Breaking the code of DNA binding specificity of TAL-type III effectors. *Science* **326**: 1509–1512.
30. Doyle, EL, Booher, NJ, Standage, DS, Voytas, DF, Brendel, VP, Vandyk, JK *et al.* (2012). TAL Effector-Nucleotide Targeter (TALE-NT) 2.0: tools for TAL effector design and target prediction. *Nucleic Acids Res* **40**(Web Server issue): W117–W122.
31. Kim, JS, Lee, HJ and Carroll, D (2010). Genome editing with modularly assembled zinc-finger nucleases. *Nat Methods* **7**: 91; author reply 91–91; author reply 92.
32. Miller, JC, Holmes, MC, Wang, J, Guschin, DY, Lee, YL, Rupniewski, I *et al.* (2007). An improved zinc-finger nuclease architecture for highly specific genome editing. *Nat Biotechnol* **25**: 778–785.
33. Szczepek, M, Brondani, V, Büchel, J, Serrano, L, Segal, DJ and Cathomen, T (2007). Structure-based redesign of the dimerization interface reduces the toxicity of zinc-finger nucleases. *Nat Biotechnol* **25**: 786–793.
34. Doyon, Y, Vo, TD, Mendel, MC, Greenberg, SG, Wang, J, Xia, DF *et al.* (2011). Enhancing zinc-finger-nuclease activity with improved obligate heterodimeric architectures. *Nat Methods* **8**: 74–79.
35. Ramalingam, S, Kandavelou, K, Rajenderan, R and Chandrasegaran, S (2011). Creating designed zinc-finger nucleases with minimal cytotoxicity. *J Mol Biol* **405**: 630–641.
36. Söllü, C, Pars, K, Cornu, TI, Thibodeau-Beganny, S, Maeder, ML, Joung, JK *et al.* (2010). Autonomous zinc-finger nuclease pairs for targeted chromosomal deletion. *Nucleic Acids Res* **38**: 8269–8276.
37. Guo, J, Gaj, T and Barbas, CF 3rd (2010). Directed evolution of an enhanced and highly efficient FokI cleavage domain for zinc finger nucleases. *J Mol Biol* **400**: 96–107.

38. Szymczak, AL, Workman, CJ, Wang, Y, Vignali, KM, Dilioglou, S, Vanin, EF *et al.* (2004). Correction of multi-gene deficiency *in vivo* using a single 'self-cleaving' 2A peptide-based retroviral vector. *Nat Biotechnol* **22**: 589–594.
39. Zhao, P, Xu, L, Ait-Mou, Y, de Tombe, PP and Han, R (2011). Equal force recovery in dysferlin-deficient and wild-type muscles following saponin exposure. *J Biomed Biotechnol* **2011**: 235216.
40. Ma, K, Mallidis, C, Bhasin, S, Mahabadi, V, Artaza, J, Gonzalez-Cadavid, N *et al.* (2003). Glucocorticoid-induced skeletal muscle atrophy is associated with upregulation of myostatin gene expression. *Am J Physiol Endocrinol Metab* **285**: E363–E371.
41. Bedell, VM, Wang, Y, Campbell, JM, Poshusta, TL, Starker, CG, Krug, RG 2nd *et al.* (2012). *In vivo* genome editing using a high-efficiency TALEN system. *Nature* **491**: 114–118.
42. Carlson, DF, Tan, W, Lillico, SG, Stverakova, D, Proudfoot, C, Christian, M *et al.* (2012). Efficient TALEN-mediated gene knockout in livestock. *Proc Natl Acad Sci USA* **109**: 17382–17387.
43. Fahrenkrug, SC *et al.* (2012). Gene inactivation and nonmeiotic allele introgression in livestock species using talens. *Reproduction, Fertility, and Development* **25**: 318.
44. Menconi, M, Gonnella, P, Petkova, V, Lecker, S and Hasselgren, PO (2008). Dexamethasone and corticosterone induce similar, but not identical, muscle wasting responses in cultured L6 and C2C12 myotubes. *J Cell Biochem* **105**: 353–364.

Supplementary Information accompanies this paper on the Molecular Therapy–Nucleic Acids website (http://www.nature.com/mtna)